Manifold Learning Method with OD Matrix as Latent Variables and Surrogate Modeling for Pedestrian Network Design

INU021002

Mizuki Ogawa
ogawa@bin.t.u-tokyo.ac.jp

Eiji Hato
hato@bin.t.u-tokyo.ac.jp

Kenta Ishii
kenta.ishii.py@hitachi.com

Abstract

This paper focuses on pedestrian behavior and attempts to construct a method to estimate Origin-Destination traffic distribution and route choice parameters simultaneously. In the previous estimation methods, it is not easy to guarantee the uniqueness of the estimated solution because the objective function is set individually. In this paper, we propose an estimation method that guarantees the uniqueness of the solution by finding the nearest point between the observed manifold and the model manifold by introducing manifold learning, which is a field of information geometry. Moreover, we conducted numerical experiments to confirm the stability of the solution using the proposed method and the previous estimation method. In addition, we developed a surrogate model to speed up the Pareto frontier search, a set of Pareto solutions, to deal with the sizeable computational load of the network design problem based on the estimated parameters. In a study of a park development plan for an actual site, we achieved a significant speedup over the usual computation time by having a feed-forward neural network learn network patterns as input and objective function values as output.

INTRODUCTION

The prolonged period of COVID-19 is changing the way urban space is being used, as people are changing their behaviors by restricting self-restraint movement(Sakai et al. (*1*)). Thus, while the reallocation of open spaces for distance is becoming more critical, there is an increasing need for flow prediction based on real-time measurements of human flow and density.

In order to understand the actual state of movement in urban space and to clarify the effects of policies, it is necessary to describe dynamic activity patterns based on partial observation information from various sensors(Hato (*2*),Oyama and Hato (*3*)).

At the same time, it is essential to estimate the OD matrix, which is an input variable for the allocation model. Based on the accumulation of many studies on OD estimation, we propose a new methodology for the optimal design of urban spaces by constructing a simultaneous estimation method for the parameters of the behavioral model.

However, the parameters of the behavioral model and the OD matrix of pedestrians are nested in each other, and it is theoretically and allegorically challenging to estimate them uniquely. In this study, we propose an estimation method that theoretically guarantees the uniqueness of the solution by treating the OD matrix as a latent variable of the link flow using the observation manifold and treating the behavioral model as a recursive model manifold. By learning the manifold, the OD matrix and the sequential choice probabilities of links or cells are estimated simultaneously.

On the other hand, it is necessary to perform a multidimensional evaluation for a vast number of combinations to design cities to meet new needs by arranging open spaces and developing networks. We can optimize through Pareto frontier analysis based on trade-off relationships among policy variables. However, it causes a significant computational load, and we need to speed up the computation speed. In recent years, there has been much interest in applying surrogate models in molecular biology and the optimal design of materials. Recently, there has been much interest in applying surrogate models in molecular biology and the optimal design of materials. In this paper, we propose a surrogate model, a new method to achieve faster computation speed by replacing the input and output of a theoretical model with an approximate model through machine learning. In this study, we aim to achieve fast policy simulation by transferring the pedestrian allocation calculation results to a neural network model to calculate approximate solutions for many policy simulation results.

In this study, the Chapter2 reviews the simultaneous estimation method of OD matrix and route choice models and the method of models with latent variables. We also review the application of surrogate models in engineering. In Chapter3, we explain the research framework and network notation, and manifolds. In Chapter4, we construct a method for simultaneous estimation of OD matrix and route choice models using manifold learning and discuss the properties of the solution. Finally, in Chapter5, we conducted numerical experiments to confirm the method's performance, followed by the estimation using real data in Chapter6. Chapter 7 explains the network design method using a surrogate model and shows its speedup. Finally, in Chapter 8, conclusions and future research.

LITERATURE REVIEW

In this chapter, we summarize the studies that have been proposed on methods for simultaneous estimation of OD matrix and route choice models and estimation methods for models with latent variables. We also review surrogate models used as alternatives to simulation and consider using them in this research.

Simultaneous estimation of OD matrix and route choice models

Liu and Fricker (*4*)constructed a method for simultaneous estimation from link flow only by dividing OD matrix estimation and link dispersion parameter estimation into two stages based on Dial allocation(Dial and Robert (*5*)).In this study, an evaluation index of the estimated values is the mean square error between the observed link traffic and the link traffic calculated using the estimated values. However, this index cannot evaluate the estimation error across the OD matrix and link cost parameters because it does not evaluate the traffic dimension of each OD. Yang et al. (*6*), Balakrishna et al. (*7*), and Wang et al. (*8*) proposed a simultaneous estimation method using generalized least squares (GLS) as the objective function, underpinned by stochastic equilibrium allocation for Dial NW. Moreover, Lo and Chan (*9*) proposed a simultaneous estimation method using Generalized Least Squares (GLS) as the objective function, assuming that OD matrix follows a normal distribution. However, these estimation methods need to prepare the information observed not only link flow but also OD matrix.

Based on these studies, it is necessary to develop an estimation method that can guarantee the uniqueness of the solution in the NW where its OD matrix is unknown. In addition, no research has proposed a simultaneous estimation method within an acceptable framework for cyclic routes to represent pedestrian stay and migration. Therefore, it is necessary to allow Markov chain allocation within the framework of simultaneous estimation methods for the analysis of pedestrian behavior. This study attempts to construct a simultaneous estimation method using the Oyama and Hato (*10*) that can express cyclic paths. In the route choice model, the Oyama and Hato (*10*) can represent the cyclic path by inserting a time-structure NW on the Recursive Logit model proposed by Fosgerau et al. (*11*), which assumes Markov chain allocation. This study attempts to construct a simultaneous estimation method using the Oyama and Hato (*10*) that can express cyclic paths.

Model estimation with latent variables

We can obtain the link flow using the current observation technology. However, we cannot observe the origin and destination points of the observed link flow due to privacy concerns. Therefore, when prior information on OD matrix is not available, simultaneous estimation of OD matrix and route choice model can be regarded as a mixture distribution estimation problem with OD matrix distribution as a latent variable.

Then, in this section, we review the estimation problem of the model with latent variables. In the transportation field, Bhat (*12*) and Vij et al. (*13*) estimated models for travel demand estimation and transportation choice, respectively, using the Expectation and Maximization (EM) algorithm to handle individual and group heterogeneity. In the observation error problem in route choice models, Oyama and Hato (*3*) dealt with the estimation problem using the links of the observed data as latent variables. We can interpret this study as a method that assumes that in the E step of the expected value calculation in the EM algorithm, we always belong to the class with the most significant probability and then perform likelihood maximization in the subsequent M step.

Thus, the EM algorithm is used for the model estimation with latent variables, but one of the challenges of this method is local solutions in the solution. For this problem, an approach using a manifold concept has been proposed from the viewpoint of information geometry Akaho (*14*).

The set $S = \{f(\mathbf{x}|\theta)\}$of random variables with parameter θ can be viewed as a space (manifold) with θ as the local coordinate system. This space does not have a distance structure like Euclidean space, and space may be curved. However, it can be regarded as locally Euclidean space, and the local coordinates θ reduce the dimension and represent the curved space. In this way, by

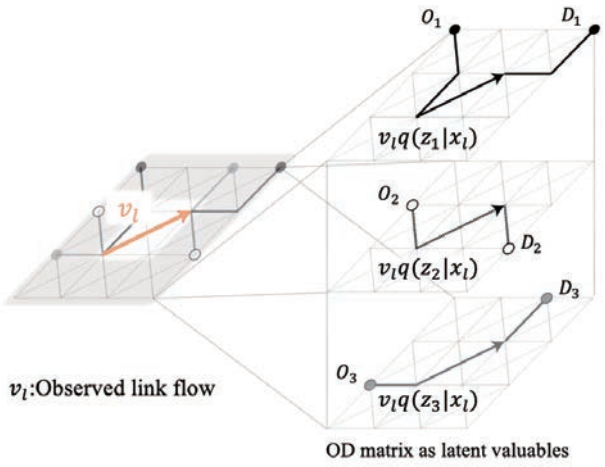

FIGURE 1 Decomposition of observed link traffic by the latent variable

fitting a local coordinate system to a high-dimensional space and reducing the number of dimensions, we can find a model manifold that best fits the observed data called manifold learning. If we consider S as a space of probability distributions, called an exponential family of distributions, a dual coordinate system, the e-coordinate system θ and the m-coordinate system η, is introduced. The observed data can be represented as a single point in the η-coordinate, and the projection of the dual coordinate system θ onto the model space M is orthogonal to the θ-coordinate. This is called the m-projection, and the projection from the model space to the observation distribution is called the e-projection. There is a deep relationship between divergence, representing the gap between probability distributions and e-projection and m-projection. It is known that e-projection and m-projection between sub-spaces of an exponential distribution family give the minimum value of divergence.

Based on the above characteristics of e-projection and m-projection, Csiszaér and Tusnaédy (*15*) defined the model manifold as the joint distribution model $p(\mathbf{x}, \mathbf{z})$ of the latent variable $\mathbf{z}$ and the observed variable $\mathbf{x}$ with the model parameter ξ as the coordinate system, and the observation manifold as the product $\hat{q}(\mathbf{x})q(\mathbf{z}|\mathbf{x})$ of the empirical distribution $\hat{q}(\mathbf{x})$ of the observed variable obtained as observation and the parameter $q(\mathbf{z}|\mathbf{x})$.They expressed the degree of separation between each manifold by KL divergence, which indicated the similarity between probability distributions. They proposed the *em* algorithm, which aims at minimizing KL divergence by alternately projecting between each manifold(Figure **??**). Moreover, Amari (*16*) showed that the *em* algorithm is equivalent to the EM algorithm when dealing with probability distribution spaces and that the em algorithm has a uniqueness of solution if there exists a duality relation where the observed data is a mixture distribution family. The estimated model is an exponential distribution family. In the transportation field, Fosgerau et al. (*17*) uses the duality of log-sum variables to generalize the model to reflect exploratory behavioral norms.

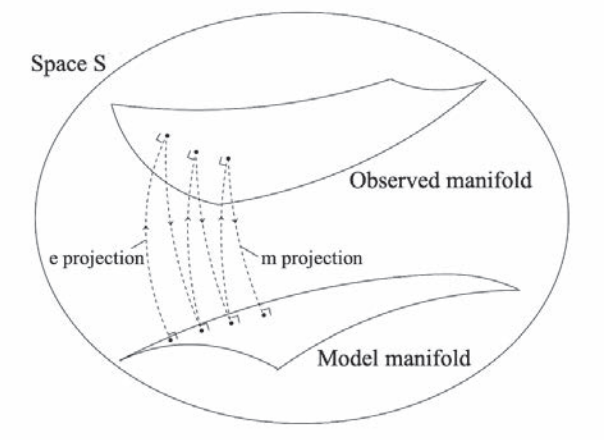

FIGURE 2 e-projection and m-projection between model manifold and observed manifold

From the above, we can understand the link flow of pedestrian by the current technology. However, it is difficult to understand the OD matrix, and there are few studies to predict the pedestrian scale OD matrix. Therefore, we developed a method for simultaneous estimation of OD matrix and route choice model using only observed link flow for a route choice model representing pedestrian. In formulating OD matrix as a latent variable, we propose a method that can guarantee the uniqueness of the solution based on manifold learning of information geometry.

Speeding up by surrogate models

The surrogate model can simulate physical phenomena as a surrogate model, and it can replace computationally extensive simulations such as stress analysis. In stress analysis, we can understand the performance of structure by inputting the geometry, decomposing the mesh, and analyzing the stress in mesh units. When we increase the mesh resolution, we can analyze with high accuracy, but the computational scale becomes very large. Thelin et al. (*18*) has developed a prediction model that uses a surrogate model to replace the FEA portion of the fatigue life simulation, which is necessary for determining jet engine components. A model that can be analyzed in real-time has been constructed by learning five shape parameters as input and the results of FEA analysis as output. Mai et al. (*19*) and Chang and Cheng (*20*) also showed that a neural network surrogate model could replace the analysis of nonlinear structures using finite element analysis, significantly reducing computational cost and guaranteeing convergence.

Surrogate models are adequate for computationally demanding and complex simulations. The network design problem(Hao (*21*),Farahani et al. (*22*),Oyama and Hato (*23*)) we attempt is to find an optimal multi-purpose solution with a large number of network patterns. The allocation computation of the Recursive Logit model(Fosgerau et al. (*11*))used in this research has a recursive computation process, which causes a huge computational load. Therefore, we propose a surrogate model using a feed-forward neural network to replace the allocation calculation.

FRAMEWORK AND NOTATIONS

In this chapter, we explain about research framework and define the variables to be used in the model, and from the viewpoint of information geometry, we define the model manifold and the observation manifold.

Research framework

We introduce the framework of this research(3). In this study, we construct a method for simultaneous estimation of OD traffic and route choice models and design a network using the obtained parameters. Then, we constructed a surrogate model to reduce the computational load of calculating enormous network patterns and allocations and accelerate the computation.

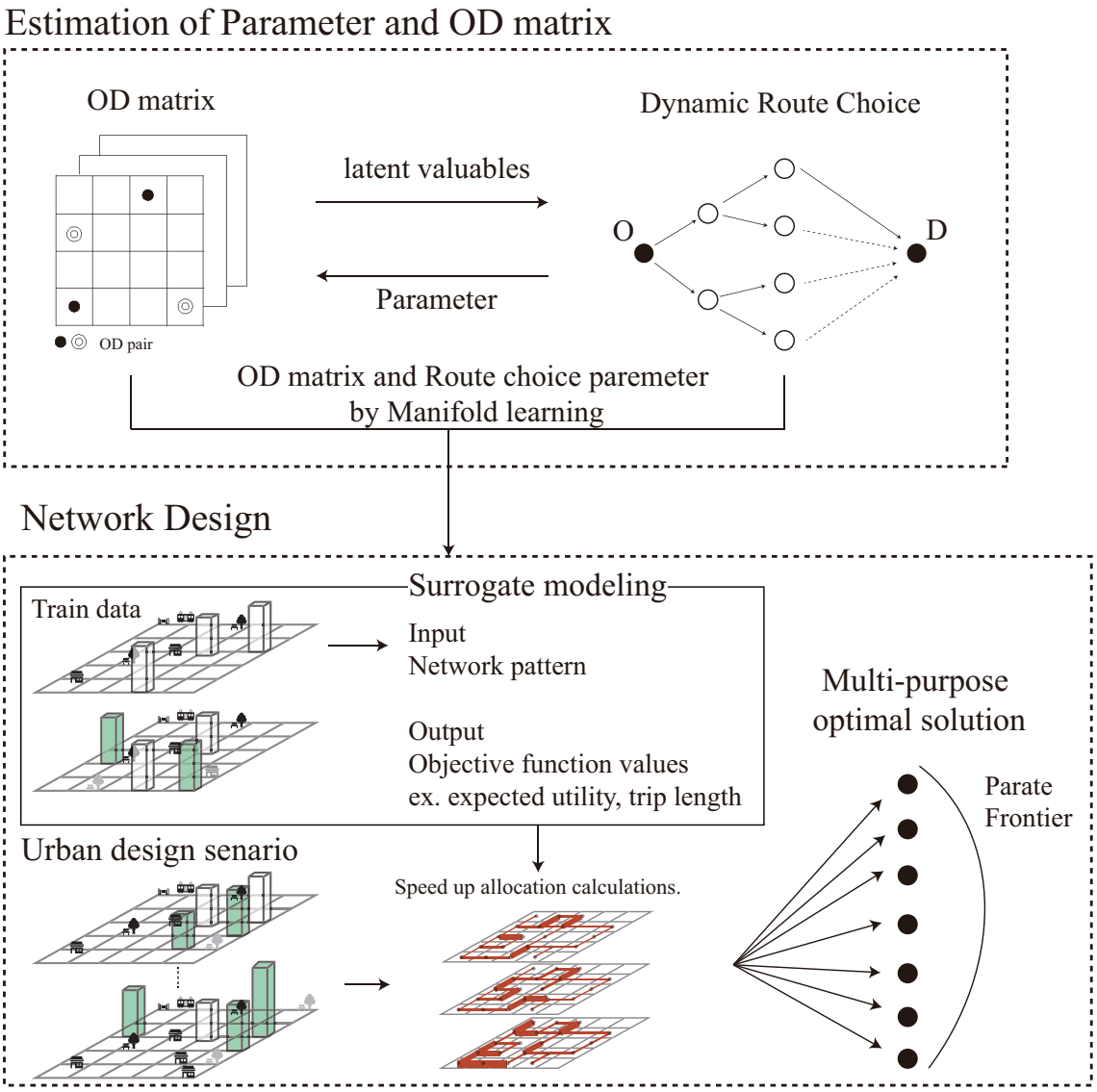

FIGURE 3 Research Framework : Simultaneous estimation of OD matrix and route choice parameters and Network Design using Surrogate model

Network notation

We define a network as a directed graph $G = (A, E)$ where the node-set is A and the link set is E (Figure 4).We define a network as a directed graph $G = (A, E)$ where the node-set is A and the link set is E.For a connected node $k \in A$, we define $A(k)$ to be the subset of nodes connected to k, and $l \in E$ to be the link connecting nodes k and a.And we define the definite term of the transition utility

from k to $a \in A(k)$ as $v(a|k)$, and its explanatory variable vector as x_l. In this paper, we describe the network without time properties for the sake of generalization, but It can also be applied to time-structured networks such as in Oyama and Hato (*10*).

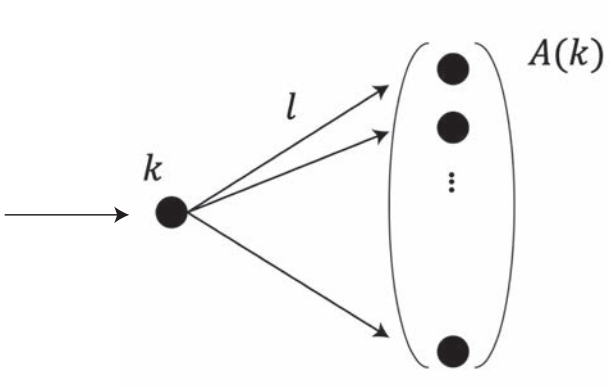

FIGURE 4 Network representation:link l connects node k and node $a \in A(k)$

Model Manifold

We formulate the link flow derived from each OD using a route choice model. Our goal is to construct a simultaneous estimation of OD matrix and route choice model that can also represent the migratory behavior of pedestrians. Therefore, we use the RL model (Fosgerau et al. (*11*)), which calculates the link choice probability based on the Markov chain allocation that can express cyclic flows, to formulate the allocated traffic volume on a logit base.

Let z be a set of OD pairs. We assume that a traveler moves between some OD pairs $z_j \in z$ by choosing nodes sequentially from the origin node $o(z_j)$ to the destination node $d(z_j)$ in a directed graph $G = (A, E)$. Let $u(a|k) = v(a|k) + \mu\varepsilon(a)$ be the instantaneous utility that the traveler can obtain when moving from the current node k to the neighboring node $a \in A(k)$. The error term $\varepsilon(a)$ is assumed to be an $i.i.d$ extreme value distribution of type I with zero mean, and μ is a scale parameter. In this case, the transition probability from node k to a is given by the MNL model as follows(1).

$$p(a|k, z_j, \theta) = \frac{\exp(v(a|k) + V^d(z_j)(a))}{\sum_{a' \in A} \exp(v(a'|k) + V^d(z_j)(a'))} \tag{1}$$

θ is the vector of explanatory variable parameters, and $v(a|k) = \theta^T x_l$. x_l is explanatory variable vector of link l. The state value function $V^d(z_j)(k)$, which is the expected downstream utility, can be formulated recursively using the Bellman equation as follows(2).

$$V^d(z_j)(k) = E[\max_a v(a|k) + V^d(z_j)(a) + \mu\varepsilon(a)] \tag{2}$$

And from the assumption of the error term, equation (2) can be transformed into a log-sum form as follows (3) .

$$V^{d(z_j)}(k) = \begin{cases} \mu \ln \sum_{a' \in A(k)} e^{\frac{1}{\mu}\{v(a|k) + V^{d(z_j)}(a)\}} & (k \neq d(z_j)) \\ 0 & (k = d(z_j)) \end{cases} \tag{3}$$

Using the RL model, we calculate the traffic volume v_{lj} of link l derived from OD pair z_j. Let $\sigma(l,j)$ denote the set of paths from $o(z_j)$ to the starting node k of link l. Each path is defined as a set of node sequences $\{s_0^r, s_1^r, ..., s_I^r, s_i^r \in A(s_{i-1}^r)\} = r \in \sigma(l,j)$ where $s_I^r = k$. Let q_j be the OD matrix of OD pair z_j. Then $v_{l,j}$ can be expressed as follows(4).

$$\begin{aligned} v_{l,j} =& q_j p(a|k,z_j;\theta) \sum_{r\in\sigma(l,j)} \prod_{i=0}^{I-1} p(s_{i+1}^r|s_i^r,z_j;\theta) \\ =& q_j \exp(\frac{1}{\mu}\{v(a|k) + V^{d(z_j)}(a) - V^{d(z_j)}(o) + \ln \sum_{r\in\sigma(l,j)} \prod_{i=0}^{I-1} p(s_{i+1}^r|s_i^r,z_j;\theta)\}) \end{aligned} \tag{4}$$

The fourth term on the right-hand side of (4) is a log-sum value that represents the expected value of the maximum utility obtained from $o(z_j)$ to node k, and can be transformed as follows(5).

$$v_{l,j} = q_j \exp(\frac{1}{\mu}\{v(a|k) + V^{d(z_j)}(a) + \bar{V}^{o(z_j)}(k) - V^{d(z_j)}(o)\} \tag{5}$$

$\bar{V}^{o(z_j)}(k)$ can be formulated recursively by applying the idea of (5) as follows(6).

$$\bar{V}^{o(z_j)}(a) = \begin{cases} \mu \ln \sum_{k'\in\bar{A}(a)} e^{\frac{1}{\mu}\{v(a|k') + \bar{V}^{o(z_j)}(k')\}} & (k \neq o(z_j))) \\ 0 & (k = o(z_j)) \end{cases} \tag{6}$$

Here, $\bar{A}(a)$ is defined as the set of nodes adjacent to node a on the graph $\bar{G}$ that inverts the directed graph G. We can express the link flow for each OD using only structural and explanatory parameters. We can apply to Dial NW, which is consistent with Vliet (*24*) by this formulation. When we apply this formulation to NW with cyclic paths, we need a negative constraint in the determinant term of utility. From the above, the simultaneous distribution of x_l is explanatory variable vector of link l x_l and OD pair z_j can be formulated as follows(7), using the parameter $\xi = \{\theta, w\}$.

$$\begin{aligned} p(x_l,z_j;\xi) =& \frac{v_{l,j}}{\sum_l \sum_j v_{l,j}} \\ =& \frac{w_j}{B(\xi)} \exp(\frac{1}{\mu}\{v(a|k) + V^{d(z_j)}(a) + \bar{V}^{o(z_j)}(k) - V^{d(z_j)}(o)\} \end{aligned} \tag{7}$$

w is a weight parameter satisfying $\sum_j w_j = 1$, and $B(\xi)$ is a normalization term, x_l is explanatory variable vector of link l and OD pair z_l. (7) can be viewed as a manifold with ξ as its coordinate system on space $S = p(x,z)$ of the entire probability distribution, which we defined as the model manifold.

Observed Manifold

In this study, we treat the link traffic of travelers in the network as an observation. Since the link flows v_l can be assumed to follow the probability of occurrence $q(x)$ of the explanatory variables of the link, the observed link flow can be expressed as $\hat{q}(x_l) = \frac{v_l}{B}$. The B represents the sum of the observable link traffic on the network. In a static network, link flow is the number of transitions between points, but in a time-structured network, we can also consider the amount of stay at a point as an observation.

When we use link traffic as an observation, the problem is that we cannot observe the OD of each traveler. Therefore, the empirical distribution obtained from the observation does not correspond to the distribution model, which is the simultaneous distribution of OD matrix

and link flow, and the OD matrix distribution becomes a latent variable. Moreover, we cannot uniquely define the observation points on space $S = p(x,z)$ of the entire probability distribution. x is explanatory variable vector and z is OD pair set. From the above, we define the manifold D by observation as follows(8).

$$D = \{\hat{q}(x)q(z|x)\} \tag{8}$$

$q(z|x)$ is an arbitrary conditional distribution, defined as a parameter corresponding to the coordinate systems z and x. Equation(8) means equivalent to defining the observation as a mixture distribution.

EM ALGORITHM AND STRUCTURE ESTIMATION

In this chapter, we focus on the divergence between the model manifold and the observed manifold and the flatness of the manifold and propose an estimation algorithm that combines structure estimation and em algorithm to guarantee the uniqueness of the converged solution.

Objective function KL divergence

In the simultaneous estimation of the OD matrix and route choice model, we define the KL divergence as the objective function, representing the degree of separation between the two manifolds. The KL divergence of two probability distributions $f(x), g(x)$ is expressed as follows(9).

$$KL(f||g) = \int f(x)[\log f(x) - \log g(x)]dx \tag{9}$$

The KL divergence is non-negative and is not strictly a distance, but it is used as the degree of separation between probability distributions. When we do not know the actual probability distribution $f(x)$, we need to estimate the actual probability distribution $f(x)$ from the observed data. In this case, we can estimate the model distribution by bringing it closer to the actual distribution, and the goal of estimation is to minimize the KL divergence. Based on the manifold defined in the previous section, we formulate the KL divergence(10).

$$KL(q(z|x)||\xi) = \sum_x \sum_z \hat{q}(x)q(z|x) \ln \frac{\hat{q}(x)q(z|x)}{p(x,z|\xi)} \tag{10}$$

Parameter $\xi = \{\theta, w\}$ is estimated by minimizing KL divergence as follows(11,12,13).

$$\tilde{\theta} = {}_{\theta}KL(q(z|x)||\xi) \tag{11}$$

$$\tilde{w} = {}_{w}KL(q(z|x)||\xi) \tag{12}$$

$$\tilde{q} = \frac{B}{B(\tilde{\xi})}\tilde{w} \tag{13}$$

em algorithm

The em algorithm (Amari (*16*)) searches for the nearest point between the observation manifold and the model manifold by alternating e-step and m-step. The e-step refers to the projection from a point on the model manifold onto the observation manifold (e-projection), and the m-step means the projection from the observation manifold onto the model manifold (m-projection). In this section, we will check the uniqueness of the solution at each step.

e step
In the e-step, we fix ξ and consider the e-projection onto the observation manifold that minimizes KL divergence with respect to $q(z|x)$ Since $q(z|x)$ is a probability distribution, it can be expressed as $\sum_{z_j \in z} q(z_j|x) = 1$. In this case, we can express the Lagrangian of the KL divergence minimization problem by using the undecided multiplier λ_l as follows(14).

$$L(q(z|x), \lambda|\xi) = \sum_{x_l \in \mathbf{x}} \sum_{z_j \in z} \hat{q}(x_l) q(z_j|x_l) \ln \frac{\hat{q}(x_l) q(z_j|x_l)}{p(x_l, z_j|\xi)} - \sum_{x_l \in \mathbf{x}} \lambda_l \Big(\sum_{z_j \in z} q(z_j|x_l) - 1 \Big) \tag{14}$$

From KKT conditions, we can transform as follows(15).

$$\frac{\partial L(q(\mathbf{z}|\mathbf{x}), \lambda|\xi)}{\partial q(z_j|x_l)} = \hat{q}(x_l) \ln \frac{q(z_j|x_l)}{p(x_l, z_j|\xi)} - \eta_l \tag{15}$$

where $\eta_l = \hat{q}(x_l) \ln \hat{q}(x_l) + 1 - \lambda_l$. We can transform equation (15) from Bayes' theorem using the relation $p(x_l, z_j|\xi) = p(z_j|x_l, \xi) p(x_l|\xi)$ as follows(16).

$$\frac{\partial L(q(\mathbf{z}|\mathbf{x}), \lambda|\xi)}{\partial q(z_j|x_l)} = \hat{q}(x_l) \ln \frac{q(z_j|x_l)}{p(z_j|x_l, \xi)} - \tau \tag{16}$$

where τ_l is a constant. In other words, when ξ is fixed, the $q(z_j|x_l)$ that minimizes the KL divergence can be obtained as follows(17,18).

$$q(z_j|x_l) = p(z_j|x_l, \xi) \tag{17}$$

$$= \frac{p(x_l, z_j|\xi)}{\sum_{z_j \in \mathbf{z}} p(x_l, z_j|\xi)} \tag{18}$$

We can see that the e-projection is uniquely determined for the observational manifolds that we deal with in this study.

m step
Next, fix $q(z|x)$ and consider the m-projection to the model manifold that minimizes the KL divergence with respect to ξ. When $q(z|x)$ is fixed, the first term of the KL divergence ((10)) is constant, and minimization of KL divergence requires maximization of the second term, $\ln p(x, z|\xi)$. Therefore, it is equivalent to considering the following maximization problem(19).

$$L(\xi|q(\mathbf{z}|\mathbf{x})) = \sum_{l \in E} \sum_{z_j \in \mathbf{z}} v_l q(z_j|x_l) \ln p(x_l, z_j|\xi) \tag{19}$$

Here, the model manifold(7) contains structural parameters and is not an exponential family of distributions. Therefore, there is no guarantee that the m-projection is uniquely determined, and the uniqueness of the solution of the em algorithm cannot be guaranteed (Amari (*16*)).

4.3 Nested pseudo em algorithm

To guarantee that the em algorithm has a single solution, we propose the nested pseudo-em algorithm (NPem), which combines the nested pseudo-likelihood algorithm (NPL) (Aguirregabiria and Mira (*25*))with the em algorithm. The parameter ξ estimated by the em algorithm satisfies Equation(17), which can be transformed by substituting it into Equation(10) as follows(20).

$$KL(q(\mathbf{z}|\mathbf{x})||\xi) = \sum_{\mathbf{x}}\sum_{\mathbf{z}} \hat{q}(\mathbf{x}) p(\mathbf{z}|\mathbf{x},\xi) \ln \frac{\hat{q}(\mathbf{x}) p(\mathbf{z}|\mathbf{x},\xi)}{p(\mathbf{x},\mathbf{z}|\xi)} \tag{20}$$

$$= \sum_{l\in E} \hat{q}(x_l) \ln \hat{q}(x_l) - \sum_{l\in E} \hat{q}(x_l) \ln p(x_l|\xi) \tag{21}$$

As a result, since the structure parameters inside the em algorithm are fixed in the Inner Algorithm, the model manifold can be treated as an exponential distribution family, and the em algorithm has a unique convergence point. If the solution converges, the convergence point is uniquely determined for the entire estimation algorithm. We will show the estimation flow of the NPem algorithm(Figure 5).

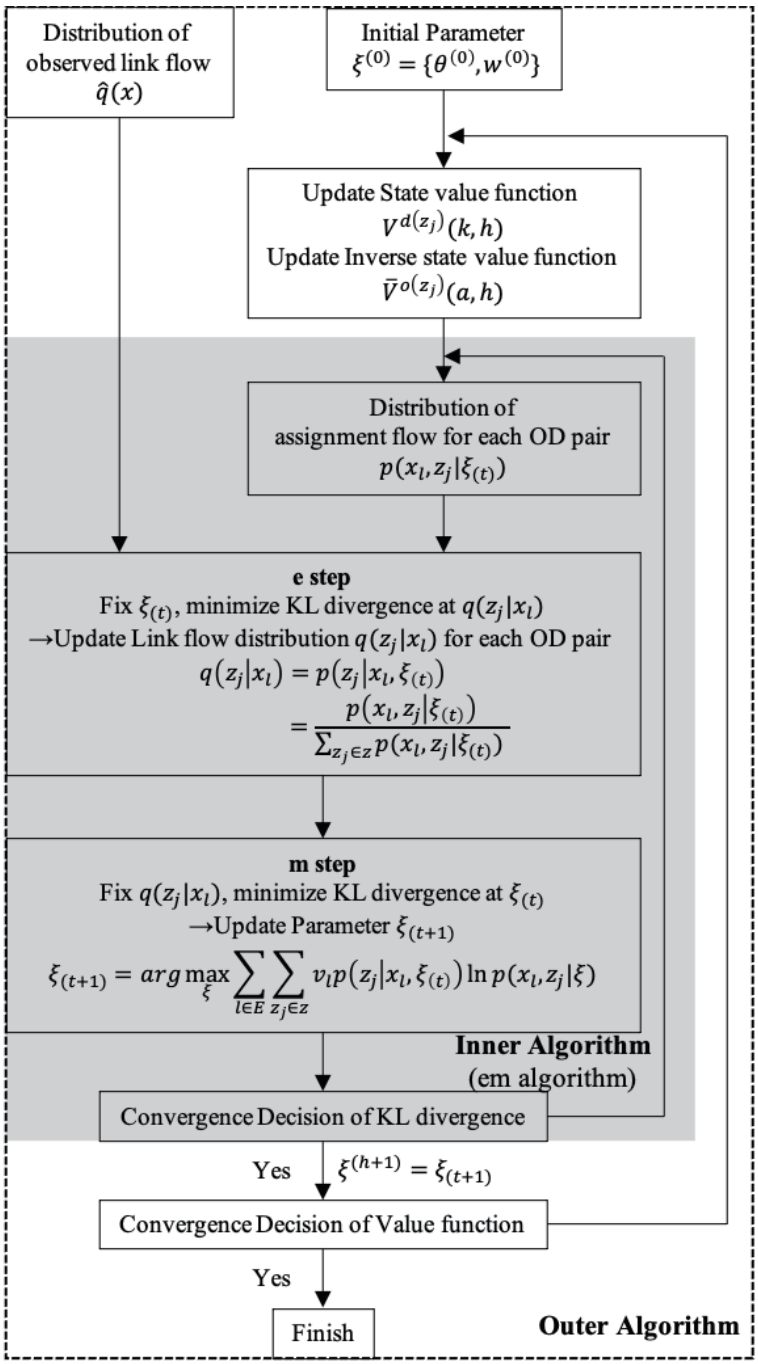

FIGURE 5 NPem algorithm is composed of Inner algorithm and Outer algorithm.

NUMERICAL EXPERIMENT

In this chapter, we confirm the stability of the estimates of the proposed method by comparing with Yang et al. (*6*) method of generalized least square (*GLS*) on the dial NW (Figure 6). In this study, we do not assume equilibrium on the NW. In the experiment, we define the instantaneous utility

obtained by a traveler's node transition as follows(22).

$$v(a|k) = \theta_{\text{length}} LC_l + \theta_{\text{shop}} DC_l \tag{22}$$

where LC_l is the link length of link l and DC_l is the store dummy of the endpoint node a of link l. The parameter $\overline{\theta} = (-1.0, 2.0)$, and we set OD pair $z_1 = (1,16), z_2 = (5,16), z_3 = (2,16), z_4 = (1,12)$ and OD matrix $q_1 = 200, q_2 = 300, q_3 = 300, q_4 = 200$.

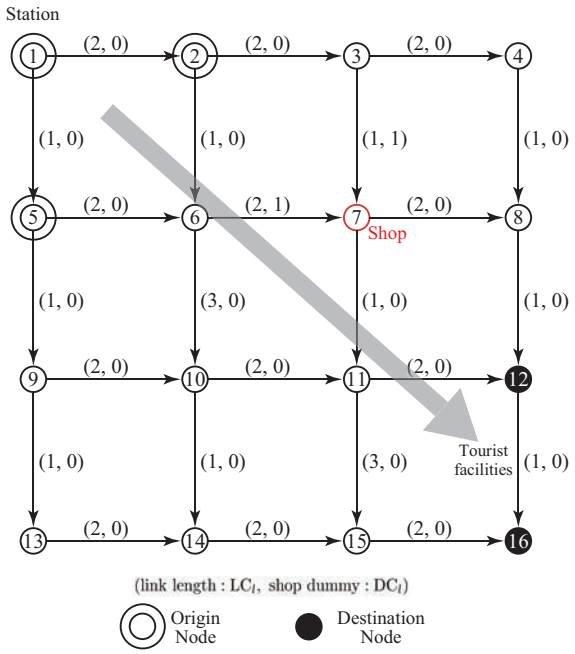

FIGURE 6 Dial NW for simulation. 3 origin and 2 destination.

We compare the mean, unbiased variance, 95% confidence interval, minimum and maximum values, and RMSE of the parameter estimates for the estimation accuracy. The RMSE is used as a parameter accurate value reproduction rate index, and the definition is as follows(23). $\hat{\Gamma}$ is the actual parameter value, Γ_i is the ith estimated parameter, and n is the number of parameters.

$$\text{RMSE}(\hat{\theta}) = \sqrt{\frac{\sum_{i=1}^{n} (\hat{\theta}_i - \theta_i)^2}{n}} \tag{23}$$

We can see in Table 1 that there is no observation error in the link flow and that the initial values of the parameters are generated with a uniform distribution for 100 trials. In the *GLS*, the mean of θ_{length} is -1.42, and there are cases where the minimum value is -8.9826, which is a significant decrease in the estimation accuracy. On the other hand, the average of θ_{length} of the proposed method is 1.0004, which means that the actual value can be estimated. RMSE, the proposed method is 0.0910 compared to 1.0608 for *GLS*, indicating a high estimation accuracy.

Table 2 shows the estimation results when there is an observation error in the link traffic. Here, we assume that the observation error follows a normal distribution with variance $\sigma_l = 5$ for all links l. When observation errors exist, the RMSE of GLS is 8.0594, while that of NPem is 6.3608, confirming the superiority of the estimation accuracy.

TABLE 1 Estimation with simulated data in dial NW

Variable	True value	Method	Mean	SD	CI 95%	Min	Max
Length	-1.00	NP_em	-1.0004	0.0018	0.0003	-1.0015	-0.9887
		GLS	-1.4200	1.5110	0.2961	-8.9826	-0.9994
Shop	2.00	NP_em	1.9980	0.0058	0.0011	1.9931	2.0200
		GLS	1.9809	0.0644	0.0126	1.7634	2.0013
OD1	200	NP_em	199.90	0.5076	0.0994	199.57	203.23
		GLS	198.81	4.0614	0.7960	184.97	200.24
OD2	300	NP_em	299.89	0.2494	0.0488	299.52	300.59
		GLS	300.99	3.3748	0.6614	299.87	312.42
OD3	300	NP_em	300.14	0.0452	0.0885	298.14	300.51
		GLS	298.95	3.5661	0.6989	286.70	300.17
OD4	200	NP_em	200.10	0.4229	0.0828	197.59	200.38
		GLS	201.75	5.9140	1.1591	199.71	221.77
	RMSE	NP_em	0.0910				
		GLS	1.0608				

TABLE 2 Estimation with simulated data in dial NW with observation error

Variable	True value	Method	Mean	SD	CI 95%	Min	Max
Length	-1.00	NP_em	-0.9729	0.0028	0.0005	-0.9752	-0.9524
		GLS	-1.3943	1.4676	0.2876	-12.4856	-0.9908
Shop	2.00	NP_em	1.8713	0.0058	0.0011	1.8633	1.9036
		GLS	1.9442	0.0550	0.0108	1.7509	2.0015
OD1	200	NP_em	203.77	0.8177	0.1603	202.86	209.46
		GLS	211.00	18.2249	3.5720	167.30	222.93
OD2	300	NP_em	286.05	0.2344	0.0459	285.55	286.57
		GLS	303.82	2.7044	0.5301	302.92	316.18
OD3	300	NP_em	306.05	0.5357	0.1050	302.70	306.64
		GLS	284.08	16.7921	3.2912	263.92	312.25
OD4	200	NP_em	199.35	0.6169	0.1209	194.86	199.78
		GLS	199.23	7.2418	1.4194	194.77	228.89
	RMSE	NP_em	6.3608				
		GLS	8.0594				

REAL DATA ESTIMATION

We estimate the actual data based on the proposed method. We use probe person data and mobile spatial statistics data in the Toyosu area in Tokyo. In order to reduce the computational load, we introduce a multi-scale network. In addition, we use a simultaneous estimation method that uses link transition probability and link flow as observations, and describe the details of the estimation method in the appendix.

Data details and network settings

we will show the details of the data used in Tables 3.

We introduce a multiscale network consisting of grids of different sizes. As NW data, we consider a multiscale network consisting of grids of different sizes. A node represents each grid, and links represent connections to neighboring grids. Each grid is connected if it is tangent to the

other grids, and the same applies to grids of different sizes (Figure 7). In this study, the explanatory variables are the distance between cells, Store area, park area, number of high-rise buildings, and dummy variables for station existence, and the length of the road in the cell(Table 4).

TABLE 3 Prove person data and Mobile Spatial data

Prove person data	data detail
Survey Term	$30^{th}Sep.2020$ $29^{th}Nov.2020$
Survey Method	Smart Phone Sensor
Survey Area	People living or working in Toyosu Area
Number of Monitors	296
Number of Trips	37920
Number of Valid Trips	37439
Mobile spatial data	**data detail**
Survey Term	1st Jul.2019 $31^{th}Jul.2020$
Survey Area	All over the country
Monitors	People use telephone of NTT docomo
Grid size	500m mesh
Time Unit	1 hour(24Class)

TABLE 4 Explanatory variables

Explanatory Variables	Overview
Distance between grids	Shortest path length between the center of PP data in the adjacent grid
Store	Area of store in each 50m grid
Park	Area of park in each 50m grid
High building	Number of building over 20th floor in each 50m grid
Station	Number of Station in each 50m grid
Road length	Road length in the cell divided by the cell area

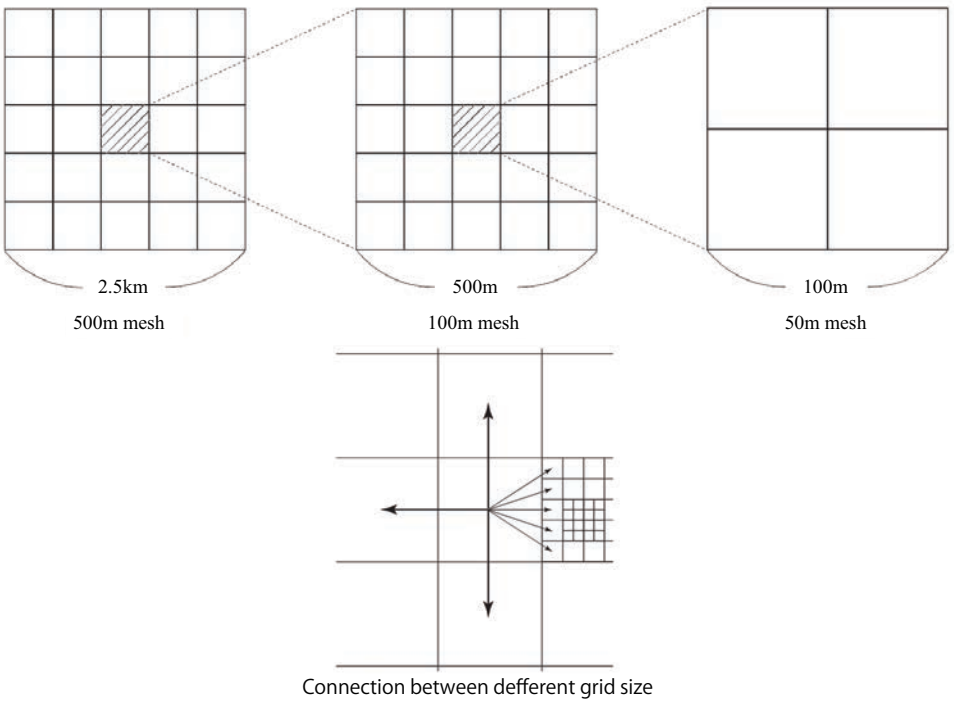

FIGURE 7 Multi-scale network and connection between different grid size

Estimation Result

We show in Table 5 the estimation results using the mobile spatial statistics data for each period and the transition probabilities obtained from the PP data. The distance between the cells parameter is negative in all periods, and the t-value is also significant. The store parameter is negative from 7:00 to 11:00, while it is positive at 12:00, 15:00, 18:00, and 20:00. It means that while the parameter is negative during commuting and work hours, it is positive after work hours, indicating that the attractiveness of the facility changes with time. The park parameter is estimated to be significantly positive at 8, 16, 18, and 22 o'clock, indicating that parks improve travel comfort even during commuting hours. Therefore, it is essential to consider people's behavioral choices that change with time.

TABLE 5 Estimation result at each hour

\time	7	8	9	10	11	12	13	14	15	16	17	18	19	20	21	22	23
Parameter	estimation value (t-value)																
Distance	-7.27	-7.26	-8.07	-8.44	-9.15	-8.05	-7.69	-7.69	-8.21	-7.79	-8.30	-7.10	-9.56	-8.74	-8.52	-7.42	-8.05
$[\theta_{length}]$	(-5.81)	(-5.53)	(-5.36)	(-7.25)	(-5.93)	(-5.42)	(-6.84)	(-6.84)	(-5.09)	(-9.38)	(-5.52)	(-5.63)	(-6.35)	(-5.74)	(-5.31)	(-5.77)	(-5.19)
Store	-1.65	-1.02	-0.61	-1.56	-0.07	0.24	-1.35	-1.35	0.49	-1.56	1.50	0.18	-0.75	1.64	-0.09	-0.26	0.29
$[\theta_{store}]$	(-2.29)	(-0.87)	(-0.32)	(-1.65)	(-0.02)	(0.10)	(-1.78)	(-1.78)	(0.26)	(-1.55)	(1.86)	(-)	(-0.81)	(1.27)	(-0.05)	(-0.55)	(0.14)
Park	-0.03	0.12	-0.02	-0.03	0.01	0.05	-0.01	-0.01	-0.31	0.10	0.06	0.15	-0.11	0.06	-0.27	0.13	-0.24
$[\theta_{park}]$	(-0.29)	(2.32)	(-0.09)	(-0.13)	(0.05)	(0.34)	(-0.13)	(-0.13)	(-0.91)	(3.97)	(0.81)	(6.32)	(-0.43)	(0.71)	(-0.74)	(4.83)	(-0.72)
Building	1.68	0.39	0.75	0.64	0.68	0.70	1.21	1.21	0.28	-0.03	0.08	0.23	0.70	0.38	0.60	0.17	0.14
$[\theta_{building}]$	(1.69)	(0.72)	(0.51)	(0.54)	(0.62)	(0.60)	(1.23)	(1.23)	(0.20)	(-0.02)	(0.09)	(0.53)	(0.63)	(0.30)	(0.44)	(0.36)	(0.10)
Station	0.55	0.32	0.36	0.46	0.23	0.22	0.53	0.53	0.13	0.39	-0.02	0.12	0.33	-0.07	0.20	0.39	0.25
$[\theta_{station}]$	(3.08)	(1.24)	(1.09)	(2.49)	(0.45)	(0.49)	(3.01)	(3.01)	(0.40)	(1.79)	(-0.12)	(1.13)	(1.90)	(-0.28)	(0.55)	(2.32)	(0.64)
Road	-1.79	-1.23	-1.07	-1.33	-0.60	-0.65	0.53	-1.70	-0.37	-1.08	0.11	-0.51	-0.99	0.44	-0.71	-1.03	-0.72
$[\theta_{road}]$	(-4.80)	(-2.25)	(-1.03	(-2.65)	(-0.35)	(-0.43)	(-3.95)	(-3.95)	(-0.36)	(-2.17)	(0.22)	(-)	(-1.70)	(0.57)	(-0.63)	(-2.11)	(-0.58)
OD1	2488.10	938.56	4669.46	3427.72	3262.76	3613.72	2660.02	2660.02	7210.59	1601.23	3770.80	1073.25	2529.57	3543.86	4815.87	1013.83	5232.84
OD2	2861.95	1205.75	5217.18	3594.16	3663.59	4184.69	2999.10	2999.09	7361.80	1705.23	4385.78	1274.89	2904.22	3691.65	5411.81	1107.167	5705.00
OD3	2537.36	1043.59	4736.16	3481.72	3285.35	3535.54	2712.18	2712.18	7233.63	1673.55	3820.67	1501.34	2549.24	3601.84	4819.12	1279.49	5252.22
OD4	3037.98	1331.94	5484.21	3803.93	3848.50	4478.87	3184.68	3184.68	7644.04	1776.02	4674.60	5625.85	3033.30	3823.82	5624.68	2695.44	5928.75
OD5	3642.56	1511.64	5383.70	3614.23	3912.93	4857.01	4000.01	4000.01	7468.50	1611.32	4944.28	1262.44	3399.69	3681.84	6513.47	1060.81	6005.75
OD6	4262.61	2013.91	6576.51	4297.92	5000.77	6122.09	4916.50	4916.50	8554.46	2033.07	5987.54	1589.62	4380.10	4095.36	7823.38	1367.89	7011.19
OD7	3121.91	1392.51	5641.30	3790.80	4054.42	4790.06	3298.85	3298.85	8049.29	1752.36	5037.32	1379.25	3226.59	4088.76	6116.29	1131.24	6193.52
OD8	3719.78	1568.69	5395.78	4072.95	3904.74	4840.61	4130.51	4130.51	7388.79	2251.69	4901.11	1274.53	3901.23	3652.53	6472.74	1095.94	5958.92
OD9	2965.36	2941.37	4201.68	2792.79	2870.58	3786.83	3200.55	3200.55	6595.87	2658.06	4514.15	1168.57	2314.80	3337.14	4819.28	1535.15	4961.88
OD10	2909.39	2941.92	4149.46	2843.34	2891.90	3801.75	3245.09	3245.09	6650.80	2711.00	4613.04	1168.26	2328.82	3312.56	4843.70	1755.09	5031.67
OD11	3752.22	1588.34	5461.61	4114.31	3661.77	4908.80	4167.90	4167.90	7509.12	2299.69	4984.21	1280.00	3937.79	3721.39	6524.03	1113.13	6009.58
OD12	5167.20	3825.68	5462.68	5628.95	6777.30	6707.38	6203.77	6203.77	7567.14	3679.07	6099.27	2820.88	5483.87	6334.97	6566.73	3240.76	6013.45
OD13	2903.40	1253.50	4977.52	3136.36	3789.53	4801.31	3080.15	3080.15	6815.45	1387.24	4950.31	1246.91	2829.44	3759.31	5354.96	1031.05	5198.24
Initial KL	59.35	61.74	62.11	64.34	67.00	63.94	64.62	64.63	63.77	65.69	61.82	62.25	67.43	62.50	61.89	63.46	65.63
Final KL	38.47	38.62	39.02	39.50	38.50	39.11	40.46	40.46	42.31	40.52	38.35	41.77	36.43	37.84	38.96	40.25	42.86

SPATIAL SIMULATION USING SURROGATE MODELS

Using the estimated model, we attempt to plan the development of parks in the Toyosu area by considering the expected utility of tourists and congestion indices. We calculate the Pareto solution set based on the park's size and its location pattern, and conduct a Pareto frontier search. However, our RL model-based allocation calculation, which expresses the migration behavior, requires recursive calculation using the Bellman equation, and the calculation cost is enormous. To solve this problem, we construct a surrogate model using a feed-forward neural network to improve the speed.

Design evaluation index

In this study, we consider the area of the park layer in the Toyosu area as a design variable. We define the objective function of the design as the expected utility of a traveler per day as follows(24)

$$\max . z_{a,1} = \frac{1}{B_{\text{all}}} \sum_{h=7}^{23} \sum_{z_j \in \mathbf{z}} \sum_{t=1}^{TS} B(h, z_j) S(t=0; h, z_j) \tag{24}$$

Where B is the sum of OD matrixs for all periods, and $B(h,z)$, is the OD matrix of OD pair z_j at time h, and $S(t=0;h,z_j)$ is the state value function of the start point of OD pair z_j at time h. We need to consider the above objective function maximization problem for all cells in the target regional network, but the computation of the optimal solution requires a large amount of computational cost. Therefore, we search for a design variable that maximizes the index considered by considering maintenance cost minimization as the objective function. The objective function of the park improvement plan $z_(b,1)$ is defined as follows(25).

$$\min . z_{b,1} = \sum_{a \in A} (n_a - n_a^{\min}) \tag{25}$$

where n_a is the park area in the cell, and $n_a^{\min}$ is the current park area in the cell. We use the network design problem as a multi-objective optimization of both equations(24 and 25) and try to improve the computational efficiency in the next chapter.

Searching solution flow

We show the searching solution flow in Figure 8. First, we make the network in which the explanatory variables of the links are changed by random sampling and calculate the value of the objective function. Next, we use the calculated objective function values and the corresponding network data as the training data for the feed-forward neural network and train the model to speed up the allocation calculation to search for the Pareto solution. In this study, we obtain the number of transitions between cells at each time and time step by performing allocation calculations based on the parameters estimated for the test network. Then, we calculate the objective function and train the model using a feed-forward neural network with the corresponding NW data as the train data. The objective function $(z_{a,1}^{(i)})$ corresponding to each network $G^{(i)}$ is regarded as a Pareto solution when the following conditions are satisfied(26).

$$\neg\{\exists G \in F, z_{a,1} \geq z_{a,1}^{(i)}\} \tag{26}$$

where, F is the set of Pareto solutions.

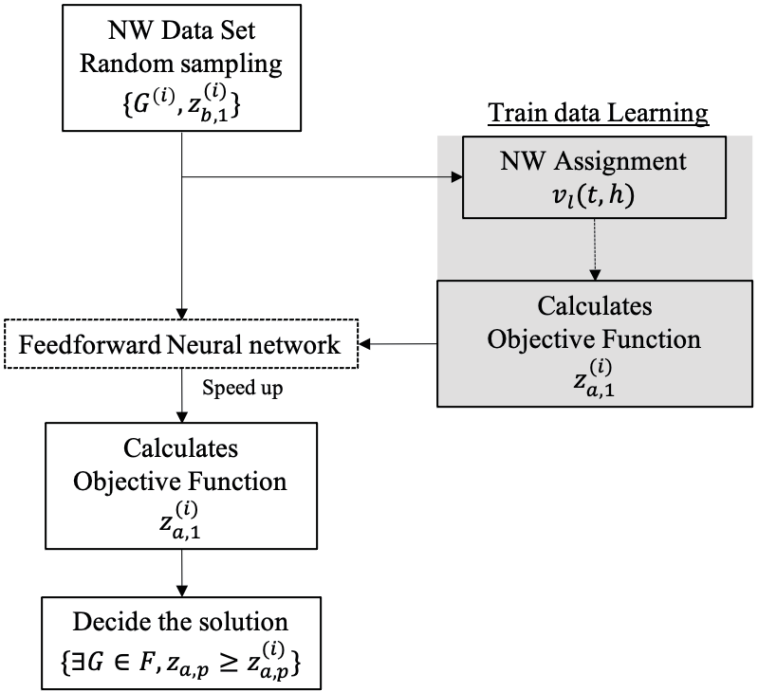

FIGURE 8 Searching Pareto solution flow using surrogate model

Training data and Model

This section creates a trainer that outputs the three objective function values described above based on the allocation results for each period from 7:00 to 23:00 in the target site.

Training data

We used the estimated OD matrix and route choice models for each period to perform allocation calculations on 6000 network data. The explanatory variables for each link are the estimated six, and the number of links is 272, so the input data is an array of 272×6. The output layer is represented by the expected utility of travelers per day z_1, the average trip length, and the *Gini* coefficient for population density considering time variation and the number of nodes in the output layer.

NN Model

First, we show the structure of the NN used in this study in Figure 9. The input layer takes an array of $272 \times 6 \times 1$ as input, and the output layer returns three outputs: expected utility, average trip length, and *Gini* coefficient for population density considering time variation. For NN learning, we use the mean squared error (MSE) defined between the prediction X_i and the correct answer $\hat{X}_i$ as the loss function. We set the learning rate to 0.001, the batch size to 20, and the number of epochs to 20. The batch size is the number of data in one set when training data is divided, and the epochs are the number of training sessions.

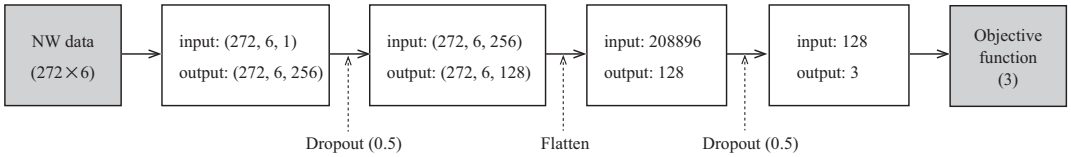

FIGURE 9 Feed-forward neural network flow

Result

Result of speed up

Figure 10 shows the training process of the NN with the loss function value on the vertical axis and the number of epochs on the horizontal axis. This figure shows the mean squared error and means an absolute error in the validation check for each epoch and the mean absolute error for the training data. It can be seen that the accuracy of the model improves with each epoch, and over-training can be avoided.

We also compared the computation time of the objective function between the surrogate model and the RL model on PC with $Intel - Core(TM)i5 - 8250UCPU1.6GHz1.8GHz$. The computation time for one time period using the estimated OD matrix and spatial choice model for 100 network data was 440 seconds. On the other hand, the NN model required only 0.09 seconds, which is 4888 times faster.

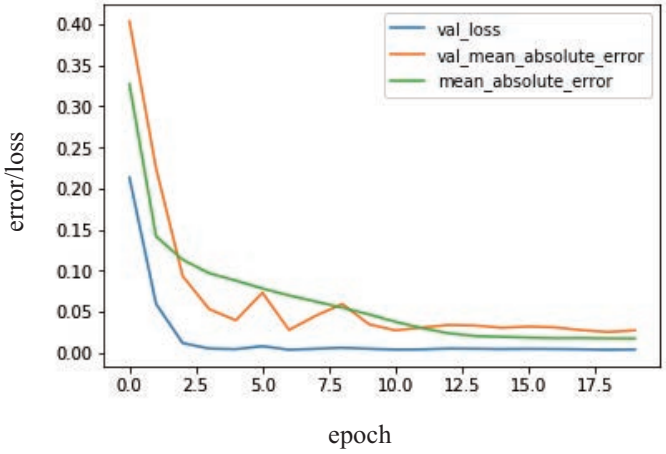

FIGURE 10 Learning process at each epoch of NN model

Result of planning park

Figure 11 shows the set of rejected NW and Pareto solutions. We can see the Pareto frontier, where the expected utility increases with the increase in the park area. From the Pareto set in Figure 7.3, we focus on Pareto solution A.

Figure 12 shows the relationship between park planning and OD points of Pareto solution *A*. The *Toyosu* and *Shin − Toyosu* direction has the most extensive park area, but the OD matrix from the *Tsukishima* direction is significant, so there is a need for park planning in the *Harumi* area. It is thought that the development located close to the activity route of travelers is practical, not only on the origin and destination points.

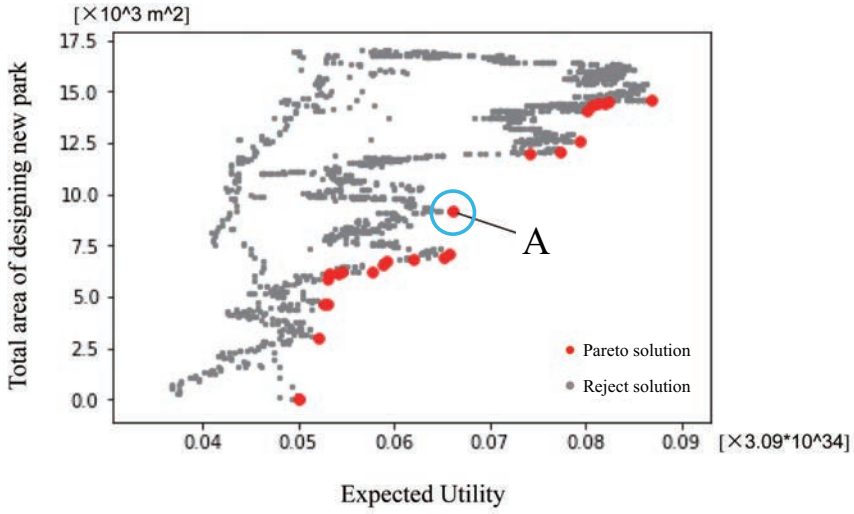

FIGURE 11 Pareto frontier with minimum park area and maximum expected utility

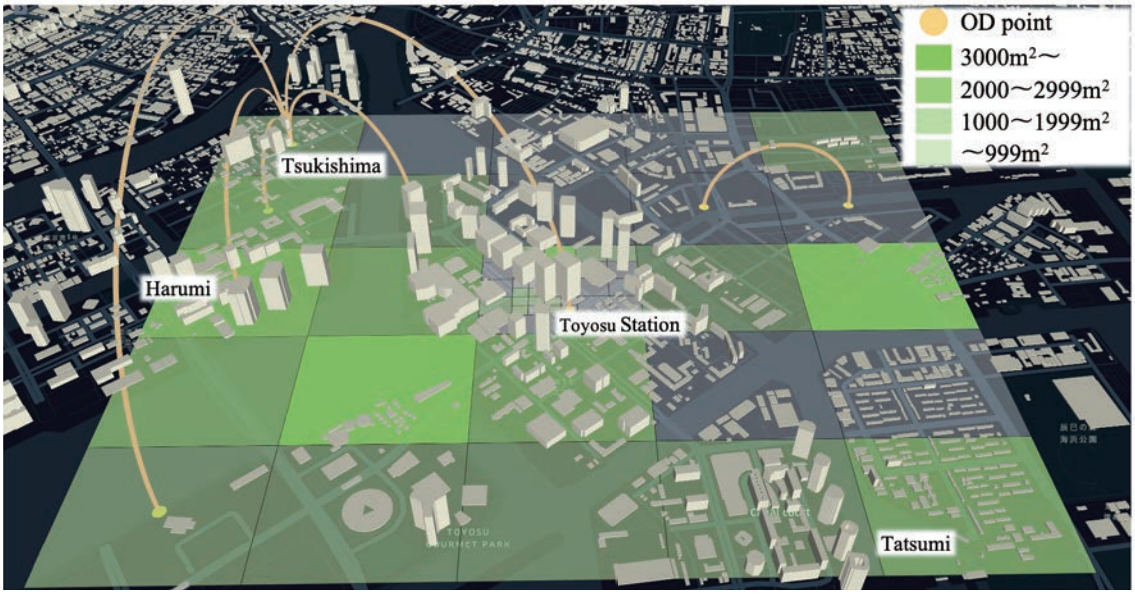

FIGURE 12 Distribution of park planning area and OD matrix in Pareto solution *A*

CONCLUSION

We proposed a simultaneous estimation of OD matrix and route choice models, using link flow or link transition probabilities as observation and a surrogate modeling approach to speed up network design.

In previous studies, estimation of the OD matrix and estimation of the parameters of the demand model has been established as different methodologies. However, we have achieved integration of the estimation methods by making the OD matrix a latent variable.

Specifically, we defined the simultaneous OD matrix and link flow as a manifold and constructed a simultaneous estimation method by combining the em algorithm and *NPL*. This method can guarantee the uniqueness of the solution from the viewpoint of information geometry. Furthermore, we compared the propose method with the conventional method and confirmed the stability of the solution and the high accuracy of the estimation from numerical experiments.

And we attempted to solve the network design by constructing a surrogate model that replaces the high computational calculation cost. Using a surrogate model that learned input network pattern and output expected utility of the traveler are learned, we achieved a computational speed 4888 times faster than the conventional framework. As a case study, we conducted a multi-objective optimization of the problem to minimize the area of park planning and maximize travelers' expected utility. We confirmed the Pareto frontier in the solution set with surrogate model.

In the future, it is necessary to perform the estimation for the whole period instead of an hourly estimation. It is a strong assumption that the values of the explanatory variables in the network are independent and travel across time. And the fusion estimation method minimized the sum of the two KL divergences, but we cannot guarantee the uniqueness of the solution of this method. It is necessary to implement the estimation with guaranteed solution using real data from data handling. Due to the prolonged COVID-19, there has been a decrease in migration behavior and OD matrix in the city, which has caused changes in the places where people are concentrated and changes in behavior. It is necessary to clarify the extent of this decrease, and to develop urban policy, urban design and evaluation for density control.

APPENDIX

Estimation method using link transition probability

We can use our simultaneous estimation method using link flow and link transition probability.

Definition manifold when we observed link transition probability

First, we formulate the simultaneous distribution of OD traffic and node transition probabilities as a model manifold. When we transition to a node $a \in A(k)$, the simultaneous distribution of its transition probability and OD pair z_j can be expressed as follows(27).

$$p(a, z_j|k;xl) = \frac{w_j p(a|k, z_j;\theta) p(k|z_j;\theta)}{p(k;\theta)} \tag{27}$$

$$= \frac{w_j p(\mathbf{x}_l;\theta)}{\sum_j \sum_a w_j p(\mathbf{x}_l;\theta)} \tag{28}$$

Next, we consider the observation manifold. We deal with the empirical distribution $\hat{q}(a|k)$ of node transition probabilities as observations. In this case, the simultaneous distribution of OD

matrix and node transition probability can be expressed as follows(29).

$$q(a,z_j|k) = \hat{q}(a|k)q(z_j|a,k) \tag{29}$$

where, $q(z_j|a,k)$ is an arbitrary conditional distribution, defined as the parameter corresponding to a,k,z_j.

Estimation method using link transition probability

The KL divergence between the observed manifold and the model manifold is defined as the objective function as follows(30).

$$KL(q(z_j|a,k)||\xi) = \sum_{k\in A}\sum_{a\in A}\sum_{z_j\in z}\hat{q}(a|k)q(z_j|a,k)\ln\frac{\hat{q}(a|k)q(z_j|a,k)}{p(a,z_j|k;\xi)} \tag{30}$$

The parameter $\xi = \{\theta, w\}$ is estimated by KL divergence(30) minimization.

$$\tilde{\theta} = \min_{\theta} KL(q(z_j|a,k)||\xi) \tag{31}$$

$$\tilde{w} = \min_{w} KL(q(z_j|a,k)||\xi) \tag{32}$$

Since this method uses transition probabilities as observations, it is impossible to convert OD traffic distribution to OD matrix. In this case, we need information about the flow rate in the NW.

Next, we consider minimizing the KL divergence by the em algorithm.

e step

In this step, we fix Γ and consider the e-projection onto the observation manifold that minimizes the KL divergence concerning $q(z_j|a,k)$. Since $q(z_j|a,k)$ is a probability distribution, we can impose the constraint that $\sum_{z_j\in z} q(z_j|a,k) = 1$, and similar to the method when the transition quantity is an observation, we can minimize the KL divergence $q(z_j|x_l)$(33).

$$\begin{aligned} q(z_j|x_l) &= p(z_j|a,k;\xi) \\ &= p(z_j|x_l,\xi) \\ &= \frac{p(x_l,z_j|\xi)}{\sum_{z_j\in \mathbf{z}} p(x_l,z_j|\xi)} \end{aligned} \tag{33}$$

m step

Next, we fix $q(z_j|a,k)$ and consider the m-projection onto the model manifold that minimizes the KL divergence with respect to ξ. This is equivalent to considering the following maximization problem(**??**).

$$L(\xi|q(z_j|a,k)) = \sum_{k\in A}\sum_{a\in A}\sum_{z_j\in \mathbf{z}} v_l q(z_j|a,k)\ln p(a,z_j|k;\xi) \tag{34}$$

By using the proposed *NPem* algorithm, we can estimate the parameters that can guarantee the uniqueness of the solution.

Fusion estimation using link flow and transition probability

In this study, we use the described PP data and mobile spatial statistics data. From the PP data, we can obtain the transition probability distribution between cells. In addition, we can obtain the number of cell states in 500m mesh units from the mobile spatial statistics data. Thus, we can obtain the number of transitions between cells in a 500m mesh NW. In this study, the multi-scale network handle meshes of 100m and 50m, so we observe the cell transition probabilities as observations for scales of 100m or less. Therefore, we will explain the estimation of fusion estimation method that uses the transition amount and transition probability as observations.

We define the objective function as the sum of the KL divergence of the link flow as an observation and the link transition probability as an observation(35).

$$\min_{\theta,q(z|a,k)} KL(q(z|x)||\xi) + KL(q(z|a,k)||\xi) \tag{35}$$

This can be interpreted as a problem of defining a model manifold with the same coordinate system and an observation manifold with the same coordinate system, and minimizing the degree of separation between each manifold, from $q(z_j \Gamma a,k) = q(z_j|x_l)$.

In the following, each step of the em algorithm for minimizing the KL divergence is explained.

e step

Fix ξ and minimize the KL divergence with respect to $q(z_j \Gamma a,k)$. We can use the Lagrangian undecided multiplier $_{k,a}$ and express it as follows(36).

$$\begin{aligned} L(q(z_j|a,k),\lambda|\xi) = &\sum_{k\in A}\sum_{a\in A}\sum_{z_j\in z} \hat{q}(a|k)q(z_j|a,k)\ln\frac{\hat{q}(a|k)q(z_j|a,k)}{p(a,z_j|k;\xi)} \\ &+ \sum_{x_l\in E}\sum_{z_j\in z} \hat{q}(x_l)q(z_j|x_l)\ln\frac{\hat{q}(x_l)q(z_j|x_l)}{p(x_l,z_j|\xi)} - \sum_{k,a\in A}\lambda_{k,a}(\sum_{z_j\in z} q(z_j|a,k)-1) \end{aligned} \tag{36}$$

From KKT conditions and $q(z_j|k,a) = q(z_j|x_l)$,

$$\frac{\partial L(q(\mathbf{z}|\mathbf{x}),\lambda|\xi)}{\partial q(z_j|x_l)} = \{\hat{q}(a|k)+\hat{q}(x_l)\}\ln\frac{q(z_j|a,k)}{p(z_j|a,k;\xi)} + \eta_{k,a} \tag{37}$$

where $\eta_{k,a}$ is a constant. From the above, when ξ is fixed, the $q(z_j \Gamma a,k)$ that minimizes the KL divergence is the following equation.

m step

Next, we fix $q(z_j \Gamma a,k)$ and consider the m-projection onto the model manifold that minimizes the KL divergence with respect to ξ. It is equivalent to considering the following maximization problem.

$$L(\xi||q(z_j|a,k)) = \sum_{k,a\in A}\sum_{z_j\in z} \hat{q}(a|k)q(z_j|x_l)\ln p(a,z_j|k;\xi) + \hat{q}(x_l)q(z_j|x_l)\ln p(x_l,z_j|\xi) \tag{38}$$

Note that this maximization problem is not a single KL divergence, but a projection problem dealing with the sum of two KL divergences, so it is difficult to discuss flatness.

REFERENCES

1. Sakai, H., M. Shimizu, T. Yoshimura, and E. Hato, Psychological Reactance to Mobility Restrictions Due to the COVID-19 Pandemic: A Japanese Population Study. *Frontiers in Psychology*, 2021.
2. Hato, E., Development of behavioral context addressable loggers in the shell for travel-activity analysis. *Transportation Research Part C: Emerging Technologies*, Vol. 18, 2010, pp. 55–67.
3. Oyama, Y. and E. Hato, Link-based measurement model to estimate route choice parameters in urban pedestrian networks. *Transportation research part C: emerging technologies*, Vol. 93, 2018, p. 62–78.
4. Liu and Fricker, Estimation of a trip table and the θ parameter in a stochastic network. *Transportation Research Part A: Policy and Practice*, Vol. 30, 1996, p. 287–305.
5. Dial and Robert, A probabilistic multipath traffic assignment model which obviates path enumeration. *Transportation research*, Vol. 5, No. 2, 1971, p. 83–111.
6. Yang, Meng, and M. GH, Simultaneous estimation of the origin-destination matrices and travel-cost coefficient for congested networks in a stochastic user equilibrium. *Transportation science*, Vol. 35, 2001, p. 107–123.
7. Balakrishna, Ben-Akiva, and Koutsopoulos, Offline calibration of dynamic traffic assignment: simultaneous demand-and-supply estimation. *Transportation Research Record*, Vol. 2003, 2007, p. 50–58.
8. Wang, Ma, Yong, K. Gong, K. C. Henricakson, M. Xu, and Y. Wang, Offline calibration of dynamic traffic assignment: simultaneous demand-and-supply estimation. *PloS one*, Vol. 11, 2016.
9. Lo and Chan, Simultaneous estimation of an origin–destination matrix and link choice proportions using traffic counts. *Transportation Research Part A: Policy and Practice*, Vol. 37, 2003, p. 771–788.
10. Oyama, Y. and E. Hato, Prism-based path set restriction for solving markovian traffic assignment problem. *Transportation Research Part B: Methodological*, Vol. 122, 2019, p. 528–546.
11. Fosgerau, Mogens, Frejinger, Emma, Karlstrom, and Anders, A link based network route choice model with unrestricted choice set. *Transportation Research Part B: Methodological*, Vol. 56, 2013, pp. 70–80.
12. Bhat, C. R., An endogenous segmentation mode choice model with an application to intercity travel. *Transportation science*, Vol. 31, 1997, p. 34–48.
13. Vij, A., A. Carrel, and J. L. Walker, Incorporating the influence of latent modal pref- erences on travel mode choice behavior. *Transportation Research Part A: Policy and Practice*, Vol. 54, 2013, p. 164–178.
14. Akaho, Information Geometry in Machine Learning. *Journal of the Society of Instrument and Control Engineers*, Vol. 44, No. 5, 2005, pp. 299–306.
15. Csiszaér and G. Tusnaédy, Information geometry and alternating minimization problems. *Statistics Decision, Supplement Issue*, , No. 1, 1984, pp. 205–237.
16. Amari, Information geometry of the EM and em algorithms for neural networks. *Neural networks*, Vol. 8, No. 9, 1995, pp. 1379–1408.
17. Fosgerau, Mogens, Melo, Emerson, Palma, A. de, Shum, and Matthew, Discrete choice and rational inattention: A general equivalence result. *Available at SSRN 2889048*, 2017.

18. Thelin, J. Salmon, S. Gorrell, S. Bunnell, G. Bird, C. Ruoti, E. Selin, and J. Calogero, sing surrogate models to predict nodal results for fatigue risk analysis. *International Journal of Fatigue*, Vol. 146, 2021.
19. Mai, J. Kang, and J. Lee, A machine learning-based surrogate model for optimization of truss structures with geometrically nonlinear behavior. *Finite Elements in Analysis and Design*, Vol. 196, 2021.
20. Chang, K.-H. and C.-Y. Cheng, Learning to Simulate and Design for Structural Engineering. *Proceedings of the 37 the International Conference on Machine Learning,PMLR*, Vol. 119, 2020.
21. Hao, V. G. . J.-K., Transit network design and scheduling: A global review. *Transportation Research Part A: Policy and Practice*, Vol. 42, 2008, p. 1251–1273.
22. Farahani, R. Z., E. Miandoabchi, W.Y.Szeto, and H. Rashidid, A review of urban transportation network design problems. *European Journal of Operational Research*, Vol. 229, 2013, p. 281–302.
23. Oyama, Y. and E. Hato, Pedestrian Activity-based Network Design based on Multi-Objective Programming. *Journal of City Planning of institute Japan*, Vol. 52, No. 3, 2017, pp. 810–817.
24. Vliet, Selected node-pair analysis in dial's assignment algorithm. *Transportation Research Part B: Methodological*, Vol. 15, 1981, p. 65–68.
25. Aguirregabiria, V. and P. Mira, Swapping the Nested Fixed Point Algorithm: A Class of Estimators for Discrete Markov Decision Models. *The Econometric Society*, Vol. 70, No. 4, 2002, pp. 1519–1543.